Journal of Applied Electrochemistry **30**: 365–370, 2000.

Analysis of PEM fuel cell stacks using an empirical current–voltage equation

D. CHU, R. JIANG and C. WALKER
US Army Research Laboratory, Sensors and Electronic Devices Directorate, Adelphi, MD 20783-1197, USA

Received 10 March 1999; accepted in revised form 29 September 1999

Key words: fuel cell stack, mass transfer, PEMFC, strip design fuel cell

Abstract

An empirical equation was developed to describe the electrode processes (activation, ohmic and mass-transfer) of PEMFC stacks over the entire current range. The potential–current and power–current curves of a strip PEMFC stack were fitted with the empirical equation under a variety of experimental humidity, temperature and stack length conditions. The concept of mass transfer impedance was defined mathematically in the present research. For the strip PEMFC stack, mass transfer impedance was only important at high currents. With decreasing humidity the mass transfer impedance increased considerably. With increasing temperature or stack cell number the mass transfer impedance increased only slightly.

1. Introduction

With the prominent features of lightweight, low cost, high-energy efficiency, high power density, non-emission and operation at low temperature, polymer electrolyte membrane fuel cells (PEMFC) have received much attention during the last 10 years [1–10]. Most of the publications concentrated on a single cell of the PEMFC or one of its components. Most recently, PEMFC stacks of various types and functions were developed [11–14]. The performance of a PEMFC stack is different than that of a single PEMFC cell. Our intent is to explore the differences of the electrode kinetic processes between PEMFC stacks and single cells, and to promote PEMFC stacks in military and civilian applications as portable power sources.

An air-breathing strip PEMFC stack is one of the newest types. There are two desirable aspects to the strip PEMFC stack. First, it produces a relatively high voltage in a compact volume and, secondly, it uses of air as the cathode reactant, resulting in a significant decrease in weight. In the strip design the weight per active area is about 40% less than that of bipolar plate stacks [14]. The air-breathing strip PEMFC stack is a two-dimensional fuel cell stack, with individual cells in the same plane [11]. This allows all of the cells to access the same reservoir of hydrogen, with the opposite face exposed to open air. However, in the investigation of the strip PEMFC stack, mass-transfer phenomena were observed when the stack was operating at high current density. This is probably because of the low oxygen concentration in air [6], low humidity or poor heat dissipation. Because it is sometimes necessary to operate at high current density, such as in an electric vehicle, understanding the electrode processes of mass transfer is important.

Since the early 1960s, several modelling studies have been carried out to elucidate cell potential against current density behaviour [5]. However, analytic expressions for the current–potential behavior have been developed only in special cases, such as when electrode reactions are either activation and ohmic or activation and mass transfer controlled. When all forms of overpotentials (activation, ohmic and mass transfer) are present, as at high current density, there are no analytical solutions for the second order differential equations. Srinivasan et al. [5] have reported mass transfer phenomena in single PEMFC cells and modelled the potential–current behaviour with an empirical equation. Our present research is to investigate the mass-transfer behaviour in the strip air-breathing PEMFC stack and to analyse the electrode kinetic processes using an empirical equation.

2. Experimental details

The air-breathing PEMFC stack was composed of 10 cells or five cells connected in series. The active area of each electrode was approximately 19 cm^2. The open circuit voltage was approximately 9.4 V for the 10-cell stack and 4.8 V for the 5-cell stack. The air supply to the cathode was by convection from environmental air. Hydrogen fuel was supplied through a sealed compartment at the anode side, and the stack was cooled naturally. The electrolyte for the single cells was prepared with a Nafion® membrane (DuPont Chemical Co.). The cathode and anode both consisted of a

commercially available catalyst (20% platinum on Vulcan XC-72 carbon from E-Tek, Inc.) and a Nafion® solution. The Nafion® membrane was positioned between the laminated cathode and anode layers to form the membrane electrolyte assembly (MEA). The MEA was processed by hot pressing at 120 °C. The catalyst loading was 0.4 mg Pt per cm^2 for both electrodes. The MEAs, metal foams, carbon cloths and metal meshes were held tightly to form single cells, which were linked in series to form a stack. A Matheson TF601 Rotameter was used for measuring the hydrogen (99.99%) flow rate. The temperature and humidity were controlled with a Tenney environmental chamber (model BTRC) and heatless dryers (model HF 200A). A Hewlett-Packard electronic load (Model 6050A) and a Hewlett-Packard multimeter were used for measuring stack current and voltage, respectively. The Tenney environmental chamber was controlled through a computer using Linktenn II software. To obtain reproducible results, all electrochemical measurements were carried out after equilibration of temperature and humidity for 2 h.

3. Results and discussion

3.1. *Typical electrochemical behaviour of mass transfer and its modelling*

Figure 1 shows a typical current–potential curve of a 10-cell strip air-breathing PEMFC stack. As current increases, voltage decreases and approaches zero volts. It is well known that the electrode polarization can be attributed to activation, ohmic and mass-transfer processes. Activation processes occur mainly at the beginning of the current–potential curve, ohmic in the middle region and mass transfer processes dominate under high current conditions. Srinivasan et al. [5, 6] used an empirical equation to describe the potential–current behaviour for a single cell. Here, we use the same equation for a PEMFC stack but define each term differently. At low and moderate currents the stack potential–current curve can be described with the following equation:

$$E_i = E_o - B\log(1000i) - R\,i \tag{1}$$

Here, E_i (V) and i (A) are the experimentally measured stack potential and current, and E_o (V) is the open circuit potential of the stack, which is equal to the sum of open circuit potentials of all the single cells connected in series. B (mV dec^{-1}) is the sum of the Tafel slope for oxygen reduction from all single cells connected in series. The R (Ω) term represents the sum of the resistance of all the single cells connected in series, such as resistances in the electrolyte membrane, which causes a linear variation of potential with current. The top curve in the Figure 1 is the computer-calculated result with Equation 1, which deviates from the experimental points at higher currents.

The entire current range of the current–potential curve can be described as

$$E_i = E_o - B\log(1000i) - Ri - i_m m\exp(ni_m) \tag{2}$$

$$i_m = i - i_d \quad \text{for } i > i_d \tag{3}$$

$$i_m = 0 \quad \text{for } i \le i_d) \tag{4}$$

Here, i_d (A) is the smallest value of current that causes the voltage to deviate from linearity in Figure 1. The value of i_d can be obtained from the experimental i/V curve or from the calculated curve with Equation 1. The m (Ω) and n (A^{-1}) terms in Equation 2 are mass-transfer parameters, which can be obtained by fitting the measured potential–current curve with computer simulation.

Equation 2 gives an excellent fit of the current–potential curves over the entire range of current. For instance, the bottom line shown in Figure 1 is the computer-calculated curve with Equation 2, which accurately fits the experimental points. The two lines calculated in Figure 1 both give the same values of E_o, B and R. Equation 2 was used to analyse all subsequent experimental data.

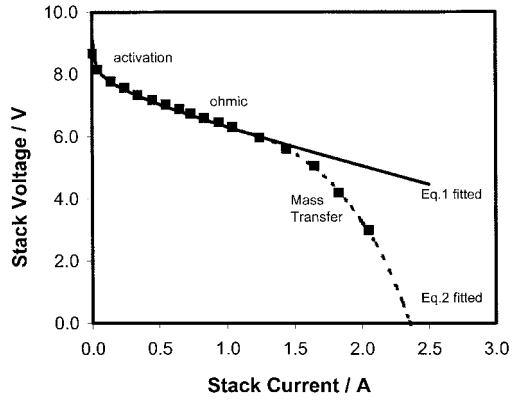

Fig. 1. Typical potential–current behaviour of a strip PEMFC stack (10 cells) with mass-transfer limitation. Points are experimental measurements and lines are computer fitted curves with Equations 1 and 2.

3.2. *Effect of humidity*

Figure 2 shows the potential–current curves and power–current curves for the strip PEMFC stack operating at various humidity levels. The lines are fitted to the experimental points with Equation 2. Voltage and power decreased with percentage RH (relative humidity), which implies that mass-transfer controlled processes become more pronounced at low humidity. The power–current curves show a peak as current is increased. For 90% and 70% RH, the maximum power was 8.3 W and 6.5 W, respectively. The kinetic parameters were obtained from computer fitting and are listed

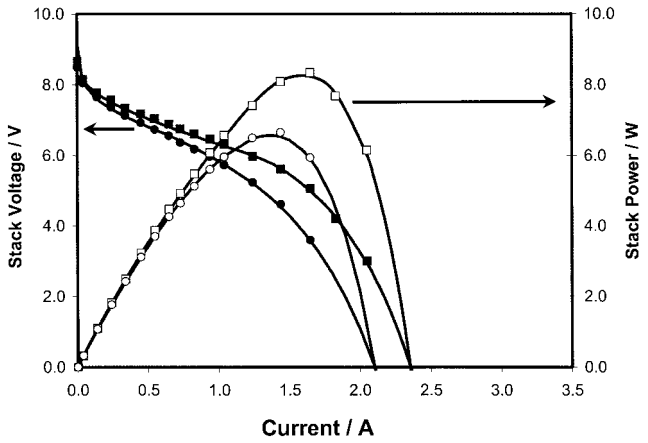

Fig. 2. Humidity effect on the polarization behaviour of the strip PEMFC stack (10 cells) at constant temperature (30 °C). Points and lines are experimental data and computer fitted curves, respectively. Key: (■) E (V), 90% RH; (●) E (V), 70% RH; (□) P (W), 90% RH; (○) P (W), 70% RH.

in Table 1. As humidity increases the B and R values both decrease, but the i_d value increases. The n value was kept constant during each calculation. Here we define another kinetic parameter, the mass-transfer impedance (R_m), to analyse the electrode processes,

$$R_m = \Delta E/i = [i_m m \exp(n i_m)]/i \quad (5)$$

In this study we only use the m and n parameters to obtain the best fit with the experimental points and we use Equation 5 to calculate the mass transfer impedance beyond the range of experimental data. Figure 3 shows the calculated mass transfer impedance at 70% RH and 90% RH. At a lower humidity there was a much larger mass-transfer impedance. The mass-transfer impedance starts from zero and increases very quickly with current for both humidity conditions.

3.3. *Performance maximization*

The performance of the strip PEMFC was maximized under the best humidity conditions: the hydrogen gas was introduced into the stack through a gas bubbler bottle and the stack body was covered with a wet cloth paper to keep humidity at saturation. Figure 4 shows the potential–current and power–current curves obtained from experimental data (points) and from computer calculations (solid lines). Compared with the condition of 90% RH, the maximized curves show

Table 1. Electrode-kinetic and mass-transfer parameters for the strip PEMFC stack at different humidity conditions
Temp. 30 °C (constant)

RH/%	E_o/V	B/mV dec^{-1}	R/Ω	m/Ω	n/A^{-1}	i_d/A
70	9.2	680	1.1	0.36	1.5	0.65
90	9.2	600	1.08	1.0	1.5	1.34
100	10.0	670	1.25	0.20	1.5	1.83

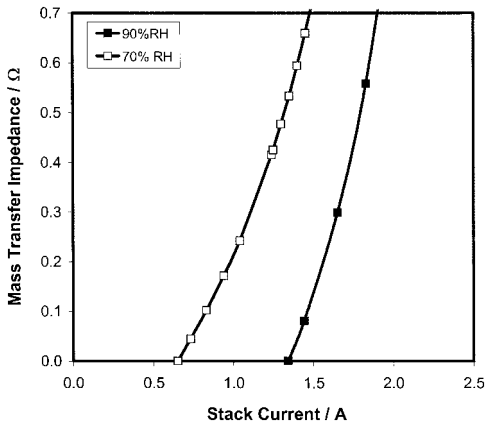

Fig. 3. Mass transfer impedance against stack current at 70% RH and 90% RH (at 30 °C). Key: (■) 90% RH; (□) 70% RH.

better performance. The peak power for the maximized condition reached about 11 W, which is about 3 W more than that at 90% RH. The plot of mass transfer impedance against stack current with and without humidity maximization is shown in Figure 5. The maximized curve has a much smaller R_m value than that at the 90% RH condition. Initially, mass transfer impedance differs little for the two curves (only a 0.4 A current difference), but quickly the difference becomes large (~1.5 A difference). The electrode kinetic parameters for the maximized condition are also shown in Table 1.

3.4. *Effect of temperature*

Figure 6 shows the potential–current and power–current curves for a series of environmental temperatures. At 10 °C the potential–current curve is fitted well using Equation 1, which implies that the electrode processes are mainly controlled by activation and ohmic events. At 30 °C and 50 °C, Equation 2 must be used to obtain

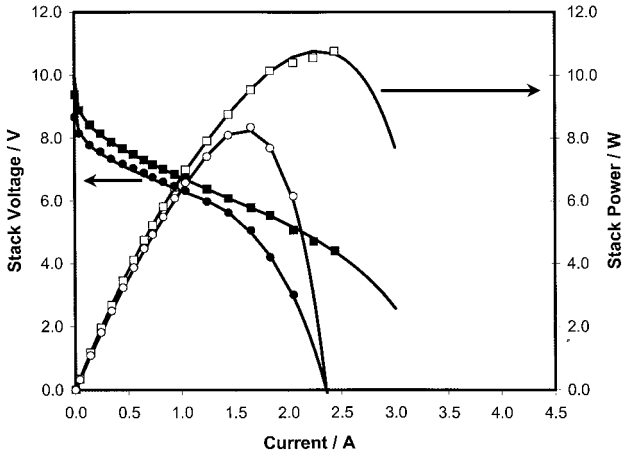

Fig. 4. Performance of a strip PEMFC stack (10 cells) with and without humidity maximization. Points and lines are experimental data and computer fitted curves, respectively. Key: (■) E (V), maximized humidity; (□) P (W), maximized humidity; (●) E (V), 90% RH; (○) P (W), 90% RH.

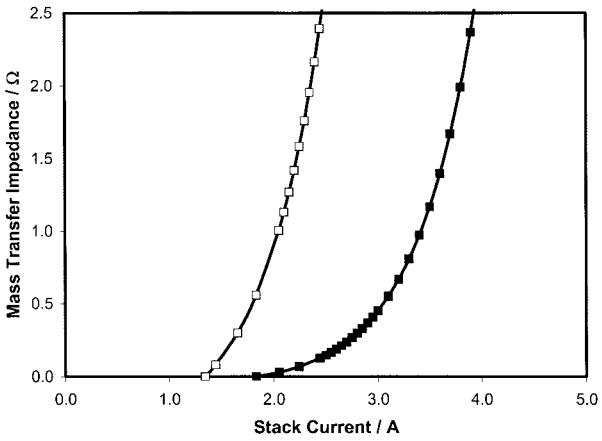

Fig. 5. Mass transfer impedance against stack current with and without humidity maximization for a strip PEMFC stack. Key: (□) 90% RH; (■) maximized humidity.

the best fit with the experimental points. It is not surprising that the mass transfer impedance seems to increase with temperature. For the initial and middle current ranges, the highest temperature produces the highest voltage and power, but at the high current range the lower temperature delivers the larger voltage and power. The electrode kinetic parameters obtained at different temperatures are shown in Table 2. The parameters at 30 °C and 50 °C are only slightly different. Plots of mass transfer impedance against stack current at 30 °C and 50 °C are shown in Figure 7. The two curves show essentially no separation (~0.1 A current difference). When the external (environmental) temperature increases, the internal stack temperature will also increase because of *IR* heating effects within the stack itself. If heat dissipation in the stack is not rapid, dehydration of the polymer electrolyte membrane and other electrode components may occur, increasing mass transfer impedance.

3.5. *Heat-transfer in the strip PEMFC stack*

To explore the internal temperature of the stack, a thermocouple was positioned inside the stack. Figure 8 shows the internal temperature variation with time under constant current operation (1.04 A). Even when the external temperature was held at 30 °C, the internal temperature was not constant but increased with time. At a lower humidity the internal stack-temperature increased faster because of higher electric resistance and mass-transfer impedance, which produced more heat.

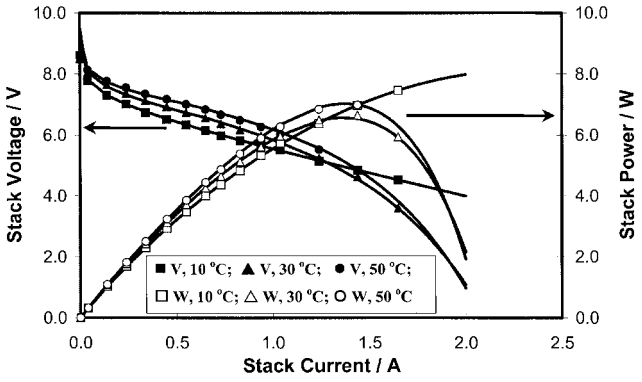

Fig. 6. Effect of air-temperature on the strip-PEMFC stack performance. Relative humidity 70%. Points and solid lines are experimental data and computer fitted curves, respectively. Key: (■) V, 10 °C; (▲) V, 30 °C; (●) V; 50 °C; (□) W, 10 °C; (△) W, 30 °C; (○) W, 50 °C.

Table 2. Electrode-kinetic and mass-transfer parameters for the strip PEMFC stack at different temperatures
Humidity 70% (constant)

T/°C	E_o/V	B/mV dec^{-1}	R/Ω	m/Ω	n/A^{-1}	i_d/A
10	9.0	700	1.35	–	–	–
30	9.2	680	1.1	0.36	1.5	0.65
50	9.3	680	0.75	0.36	1.5	0.55

3.6. *Effect of stack length*

To design a high efficiency strip PEMFC stack, it is important to understand the electrode processes for different stack lengths. Figure 9 shows the current–

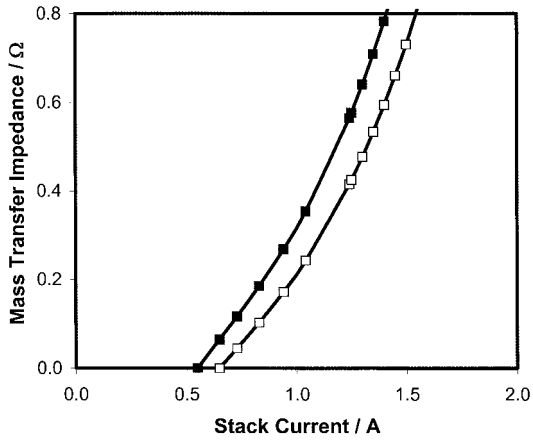

Fig. 7. Mass transfer impedance against stack current at different air-temperatures for 70% RH. Key: (■) 50 °C; (□) 30 °C.

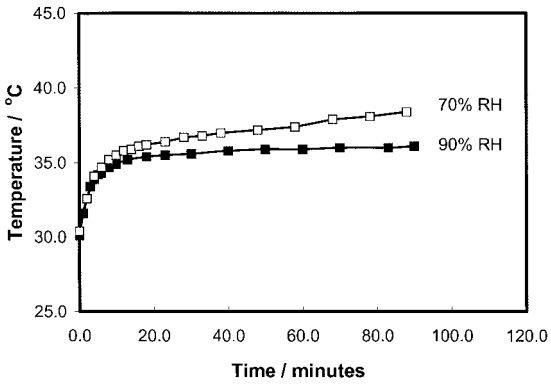

Fig. 8. Internal temperature variation with time for the strip PEMFC stack at constant current operation (1.04 A). Air temperature 30 °C (constant).

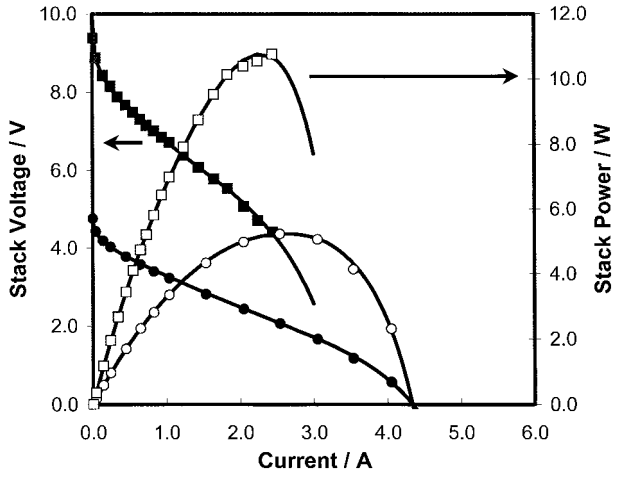

Fig. 9. Comparison of strip PEMFC performance for short (5 cells) and long (10 cells) stacks. Performance for both cells was obtained at maximized humidity condition (100% RH). Points and lines are experimental data and computer fitted curves, respectively. Key: (●) E (V), 5 cell stack; (■) E (V), 10 cell stack; (○) P (W), 5 cell stack; (□) P (W), 10 cell stack.

potential and power–potential curves for 5-cell and 10-cell stacks. The points in Figure 9 were obtained from experimental data, and the lines were drawn using Equation 2. The 5-cell stack data show much less curvature than that of the 10-cell stack. The 10-cell stack had a peak power of approximately 11 W, but the peak power for the 5-cell stack was only 5 W. Table 3 shows the kinetic parameters for the two stack designs. It is interesting that the parameters E_o, B, R and m for the 5-cell stack are about half that of the 10-cell stack, but the i_d value is about two times larger for the 5-cell stack than that for the 10-cell design. Figure 10 shows a plot of mass transfer impedance against stack current for the 5-cell and 10-cell stacks. The two curves are separated by a large gap (from 1.2 to 2.0 A). Although, the 5-cell stack has a much smaller impedance, the 10-cell stack is more efficient because the power density is larger (more than double that of the 5-cell design).

3.7. *Stability test*

In these experiments the strip PEMFC stack was operated at constant current and the voltage was measured with time, as shown in Figure 11. No voltage decrease for 120 min was observed for constant current operation at 1.54 A. However, when the current was increased to 2.05 A, the voltage was not stable, but decreased rapidly with time, probably because of poor heat dissipation and membrane dehydration.

Table 3. Electrode-kinetic and mass-transfer parameters for different lengths of strip PEMFC stacks at the maximized humidity condition

Stack length	E_o/V	B/mV dec^{-1}	R/Ω	m/Ω	n/A^{-1}	i_d/A
10 cells	10.0	670	1.25	0.20	1.5	1.83
5 cells	4.95	315	0.715	0.08	1.5	3.05

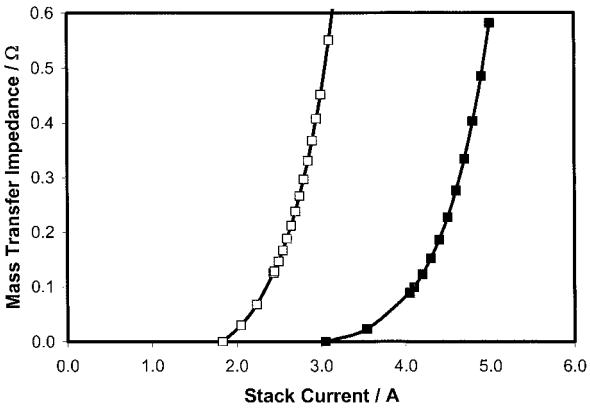

Fig. 10. Mass-transfer impedance against stack current for different stack lengths. Stack performance for both stacks was obtained at maximized humidity condition (100% RH). Key: (■) 5 cell stack; (□) 10 cell stack.

4. Conclusion

An empirical equation was developed to describe the electrode processes (activation, ohmic and mass-transfer) of a PEMFC stack over the entire current range. The potential–current and power–current curves of the strip PEMFC stack were fitted with the empirical equation under a variety of experimental humidity, temperature and stack length conditions. The concept of mass transfer impedance was defined mathematically in the present research. For the strip PEMFC stack, mass transfer impedance was only important at high currents. With a decrease in humidity, the mass transfer impedance increased considerably. With temperature changes from 30 to 50 °C, the mass transfer impedance increased slightly. At a low temperature operation, the mass-transfer impedance was small because of better heat dissipation from the stack. Increasing the total number of cells in the PEMFC strip increased the mass-transfer impedance proportionally. However, the overall power density for a 10-cell PEMFC stack was larger than that for a 5-cell stack.

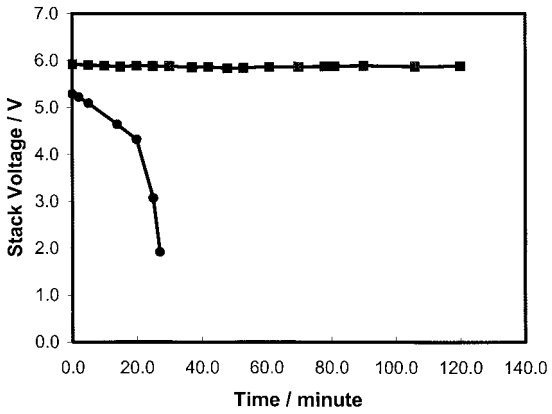

Fig. 11. Stability of the strip PEMFC stack at maximized humidity condition (100% RH). Key: (■) E, for $I = 1.54$ A; (●) E, for $I = 2.05$ A.

Acknowledgement

The authors wish to thank the Army Materiel Command for its financial support of this project.

References

1. T.F. Fuller, The Electrochemical Society Interface (Fall 1997), p. 26.
2. E.A. Ticianelli, C.R. Derouin and S. Srinivasan, *J. Electroanal. Chem.* **251** (1988) 175.
3. I.D. Raistrick, *US Patent 4 876 115* (1990).
4. M.S. Wilson and S. Gottesfeld, *J. Appl. Electrochem.* **22**, (1992) 1–7.
5. J. Kim, S.M. Lee, Srinivasan and C.E. Chamberlin, *J. Electrochem. Soc.* **142** (1995) 2670.
6. Y.W. Rho, O.A. Velev, S. Srinivasan and Y.T. Kho, *J. Electrochem. Soc.* **141** (1994) 2084.
7. H.F. OetJen, V.M. Schmidt, U. Stimming and F. Trila, *J. Electrochem. Soc.* **143** (1996) 3838.
8. M. Uchida, Y. Aoyama, N. Eda and A. Ohta, *J. Electrochem. Soc.* **142** (1995) 4143.
9. F.N. Buchi, B. Gupta, O. Haas and G.G. Scherer, *J. Electrochem. Soc.* **142** (1995) 3044.
10. M. Uchida, Y. Aoyama, N. Eda and A. Ohta, *J. Electrochem. Soc.* **142** (1995) 463.
11. J.B. Lakeman and J. Cruickshank, *in* Proceedings of the 38th Power Sources Conference, Cherry Hill, NJ (June 1998), p. 420.
12. A.C. Oliver and E. Clarke, *in* Proceedings (note [11]), p. 424.
13. L.P. Jarvice and D. Chu, *in* Proceedings (note [11]), p. 428.
14. O. Polevaya and D. Bloomfield, *in* Proceedings (note [11]), p. 416.
15. C.E. Chamberlin, P.A. Lehman, R.M. Reid and T.G. Herron, *in* 'Hydrogen Energy Process X' (edited by D. Block and T.N. Veziroglu), Proceedings of 10th World Hydrogen Energy Conference, Cocoa Beach, FL., 20–24 June (1994), Vol. 3 pp. 1659–63, International Association for hydrogen Energy, FL (1994).